

## Modeling of Cyclic Deformation of Sandstones Based on Experimental Observations

Hernandez, E. ; Naderloo, M.; Ramesh Kumar, K.; Hajibeygi, H.; Barnhoorn, A.

**DOI**

[10.3997/2214-4609.202221120](https://doi.org/10.3997/2214-4609.202221120)

**Publication date**

2022

**Document Version**

Final published version

**Published in**

EAGE GET 2022

**Citation (APA)**

Hernandez, E., Naderloo, M., Ramesh Kumar, K., Hajibeygi, H., & Barnhoorn, A. (2022). Modeling of Cyclic Deformation of Sandstones Based on Experimental Observations. In *EAGE GET 2022*  
<https://doi.org/10.3997/2214-4609.202221120>

**Important note**

To cite this publication, please use the final published version (if applicable).  
Please check the document version above.

**Copyright**

Other than for strictly personal use, it is not permitted to download, forward or distribute the text or part of it, without the consent of the author(s) and/or copyright holder(s), unless the work is under an open content license such as Creative Commons.

**Takedown policy**

Please contact us and provide details if you believe this document breaches copyrights.  
We will remove access to the work immediately and investigate your claim.

***Green Open Access added to TU Delft Institutional Repository***

***'You share, we take care!' - Taverne project***

**<https://www.openaccess.nl/en/you-share-we-take-care>**

Otherwise as indicated in the copyright section: the publisher is the copyright holder of this work and the author uses the Dutch legislation to make this work public.

## Modeling of cyclic deformation of sandstones based on experimental observations

*E. Hernandez<sup>1</sup>, M. Naderloo<sup>1</sup>, K. Ramesh Kumar<sup>1</sup>, H. Hajibeygi<sup>1</sup>, A. Barnhoorn<sup>1</sup>*

<sup>1</sup> Delft University of Technology

### Summary

---

Underground energy storage (UES) in porous and cavity reservoirs can be used to balance the mismatch between the production and demand of renewable energy. Understanding the geomechanical behaviour of these reservoirs under different storage conditions, i.e., storage frequency and fluid pressure, is key in defining their capacity and effective lifetime. This work presents an analysis performed on sandstones to unravel their geomechanical response under cyclic loading. It includes, importantly, both experimental and numerical investigations under deviatoric stress conditions below the rock dilatant cracking threshold. From the experimental point of view, axial strains and acoustic emissions indicated that inelastic strains accumulated cycle after cycle, following a decreasing rate per cycle. Four types of deformations were interpreted: elastic, viscoelastic, plastic, and cyclic-plastic. Based on these experimental results and observations, the Modified Cam-clay model was extended to account for cyclic plastic deformations and the Kelvin-Voigt model was used to model visco-elasticity. This approach can be used to study cyclic sandstone deformation's implications on subsidence, fault reactivation, and cap rock flexure, among other physical phenomena impacting a reservoir's storage capacity.

## Introduction

Storage of water, energy and other fundamental resources, in the period of surplus production, is crucial to provide secure supply in moments of shortage or high demands. The underground has proved to be a good option for storing energy-rich or energy-carrier fluids, such as hydrocarbons, hydrogen, compressed air, and cold and hot water. For instance, there are commercial applications like compressed air energy storage “CAES”, aquifer thermal energy storage “ATES” and underground gas storage “UGS”, that are able to store huge amounts of renewable or fossil energy (Snijders, 2000, Tek, 1987). All these applications are based on the injection of the mentioned fluids in underground reservoirs that can be porous-permeable rocks, salt caverns and abandoned mines. These fluids are then produced back when the production is smaller than the consumption amount. As a consequence of these injections and productions, over years, the resulting reservoir fluid pressure fluctuates cyclically, which leads to fluctuations of the effective stresses acting on the porous reservoir rock, i.e., the rock undergoes also through a cyclic loading. These cyclic loading conditions induce elastic and inelastic strains cycle after cycle in the rocks, as shown by Dietl et al., 2018 and Cerfontaine and Collin, 2018. The inelastic strains could induce caprock flexure and permanent reduction of reservoir porosity (Heinemann et al., 2021) as well as potential changes in the stress path on the fault's planes during UES. To study these possible consequences that may limit the storage capacity, constitutive models which can capture these cyclic deformations are needed. For instance, bounding surface plasticity constitutive models has been proposed to model cyclic deformation of sandstones as shown by Vermeer and de Borst, 1984 and Cerfontaine et al., 2017. Another approach for clay soils is the use of the Modified Cam-clay model “MCC” by assuming a shrinking yield surface as proposed by Carter et al., 1979. In this paper, cyclic loading experiments results on sandstones are shown, which allowed identifying the deformation mechanism presented under stress states below dilatant cracking stress threshold. Consequently, a modeling strategy for sandstone cyclic plasticity, inspired in the work of Carter et al., 1979, is proposed.

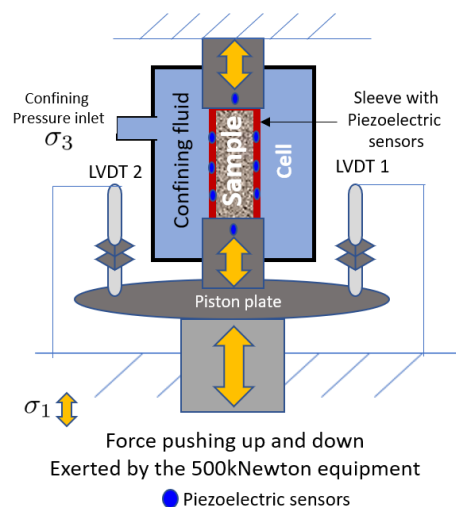


**Figure 1** Schematic of the equipment used to perform the triaxial cyclic tests. Axial strains and acoustic emissions were recorded with the LVDT and piezoelectric sensors respectively.

## EXPERIMENTAL METHODS

The triaxial cyclic tests, which consist in cycling the axial stress ( $\sigma_1$ ) while keeping constant the minimum stress ( $\sigma_3$ ), were performed to mimic the stress fluctuation during UES. A triaxial 500 kN machine equipped with piezoelectric sensors and LVDT was used to perform the cyclic tests as shown in Figure 1. Thus, axial strains and acoustic emissions were recorded. The selected rock was Red Felser sandstone (Pfaelzer Sandstein) with an average porosity of 19.6% and Young's modulus of 20 GPa at confining stress of 10 MPa. Tests were carried out imposing triangular stress waveforms under different amplitude, axial mean stress and frequencies (0.014Hz, 0.0014Hz, 0.0002Hz). The objective of the tests

was to explore early deformation at stress below the onset of dilatant cracking. Therefore, the number of cycles was limited up to 8 for constant amplitude tests and 16 for multi-amplitude tests.

## EXPERIMENTAL RESULTS

### Strain behaviour

Figure 2-a shows the total and inelastic strain response to cyclic deviatoric stress conditions ('q') for a multi-amplitude test with frequency of 0.014Hz. It can be seen that the axial strain ( $\epsilon_1$ ) is also cyclic and accumulates during the first eight cycles ( $q_{max}=48\text{MPa}$ ). This is the result of inelastic strains being generated cycle after cycle (Figure 2-b). Nevertheless, when the amplitude is reduced ( $q_{max}=30\text{MPa}$ ), no inelastic strains were recorded. It is only after increasing the deviatoric stress, to a value higher than the initial maximum stress, that inelastic strains were generated again. In addition, for test with constant mean stress and amplitude, it was measured that the lower the frequency the larger the inelastic strain. Thus, time-dependent inelastic deformation was taking place.

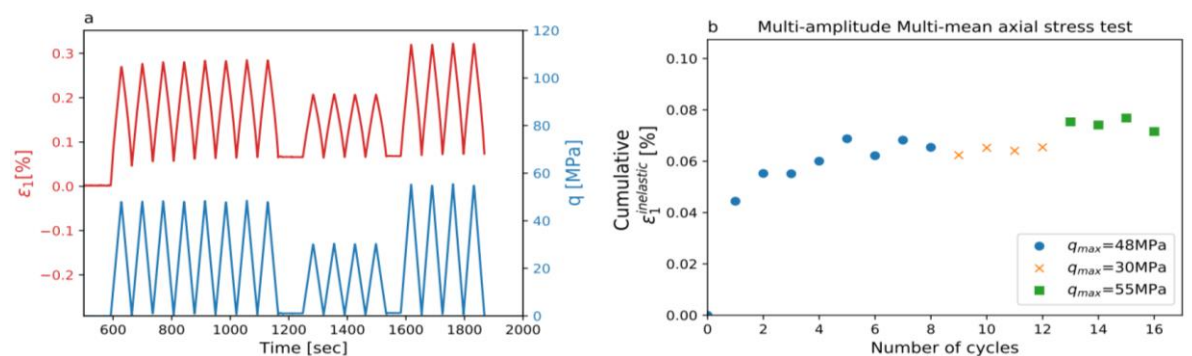


**Figure 2** Imposed Multi-amplitude cyclic loading condition and corresponding strain response (a). Cumulative inelastic strain versus number of cycles (b). Red Felser sandstone, frequency 0.014Hz.

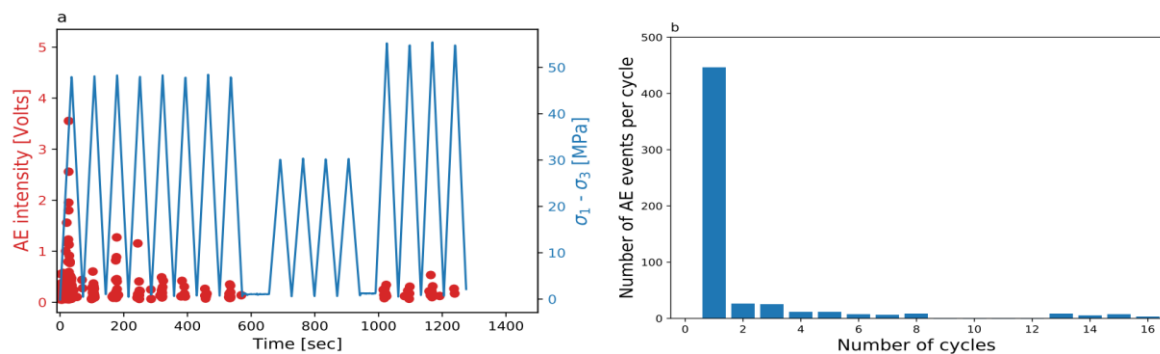


**Figure 3** Acoustic emission intensity versus time (a) and the number of acoustic events per cycle (b) during a multi-amplitude cyclic test. Red Felser sandstone, frequency 0.014Hz.

### Acoustic emissions 'AE' and cyclic deformations

In all tests, AE were recorded right after increasing the deviatoric stress in the first cycle (red dots in Figure 3-a). Nevertheless, during subsequent cycles, AE were triggered at higher stresses but lower than the applied maximum stress. In addition, the maximum intensity and number of AE were recorded in the first cycle as shown in Figures 3-a and 3-b. Then, the number of AE decreased cycle after cycle similar to inelastic strains. It was also noticed in multi-amplitude tests that inelastic strain and AE are not generated when the maximum deviatoric stress is reduced to a certain value (Figures 2-b and 3-b). In fact, AE are only triggered once a stress limit is reached, which changed with the cycles. Thus, if there is a correlation between AE and inelastic strains as mentioned by Lockner, 1993 and suggested by these experimental results, this would mean that the yield point (plasticity threshold) increases during cyclic loading.

**MODELING PROPOSAL**

Based on the experimental observations, a viscoelastic cyclic plastic model is proposed. This proposal is shown in Figure 4 and in equation 1 for triaxial conditions. Here,  $\eta_1$  is the viscoelastic viscosity,  $E_1$  and  $E_2$  are the Young's modulus of the spring and Kelvin-Voigt units respectively. For cyclic plastic deformations, an extension of Modified Cam-clay model ' $MCC_{Cyclic}$ ' is proposed based on the work of Carter et al., 1979.

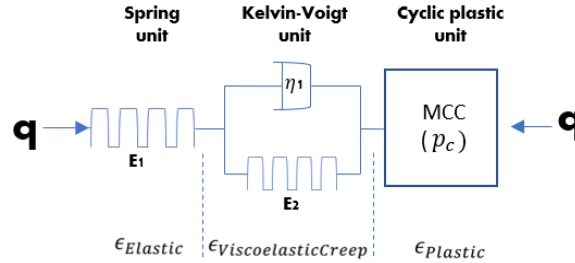


**Figure 4** Representation of the proposed viscoelastic - cyclic plastic model for deviatoric stress 'q'. Where  $p_c$  is the  $MCC_{Cyclic}$ 's over-consolidation parameter, which is a function of the cyclic stresses.

$$\epsilon_1 = \frac{q}{E_1} + \frac{q}{E_2} \left( 1 - e^{-\frac{E_2 t}{\eta_1}} \right) + MCC_{Cyclic} \quad (1)$$

The proposed  $MCC_{Cyclic}$  considers a spreading yield surface with respect to the cyclic deviatoric 'q' and pressure 'p' stresses (equation 2, where M is the slope of critical state line). This means that the size of the yield surface increases in every cyclic loading if yielding is taking place. Equation 3 rules the mentioned increase by updating the over-consolidation parameter of the yield surface ( $p_c$ ) after yielding, where  $p_l^{Max}$  is the maximum loading parameter and  $\theta$  is the cyclic parameter. For a detailed description of the MCC model the reader is referred to Carter et al., 1979.

$$f = q^2 - M^2(p(p_c - p)) \quad (2) \quad p_c^{new} = p_c^{old} \left( \frac{p_l^{Max}}{p_c^{old}} \right)^\theta \quad (3)$$

$f \geq 0 \rightarrow$  Plastic strains  
 $f < 0 \rightarrow$  Elastic strains

The main characteristics of the cyclic MCC model are:

- If  $\theta$  is equal to 1 (maximum value), the model reduces to the standard MCC model. Otherwise, cyclic inelastic strains are generated.
- As the number of cycles increases  $p_c^{new}$  becomes closer to  $p_l^{Max}$ .
- Unloading behaves elastically and the shape of the yield function remains the same (an ellipse).

**Modeling results against experimental data**

Figure 5 shows the comparison between the model and the cyclic test in terms of axial strains and inelastic strains. It can be seen that the model can forecast the inelastic strain ( $\epsilon_1^{inelastic}$ ) recorded in the first cycle as well as the decreasing rate of inelastic strain per cycle (Figure 5-b). Figure 5-c shows that the model captures the non-linear behaviour of strain caused by viscoelasticity and inelastic strain. The process to fit the model to the experimental data was as follows: First, the experimental cyclic inelastic strains were reproduced with the  $MCC_{Cyclic}$  model by adjusting the parameter  $\theta$  and assuming an initial average Young's modulus. Second, the viscoelastic viscosity and Young's modulus were adjusted to fit the total strain while holding constant the cyclic inelastic strains. This was done iteratively until convergence of Young's modulus was obtained between both models.

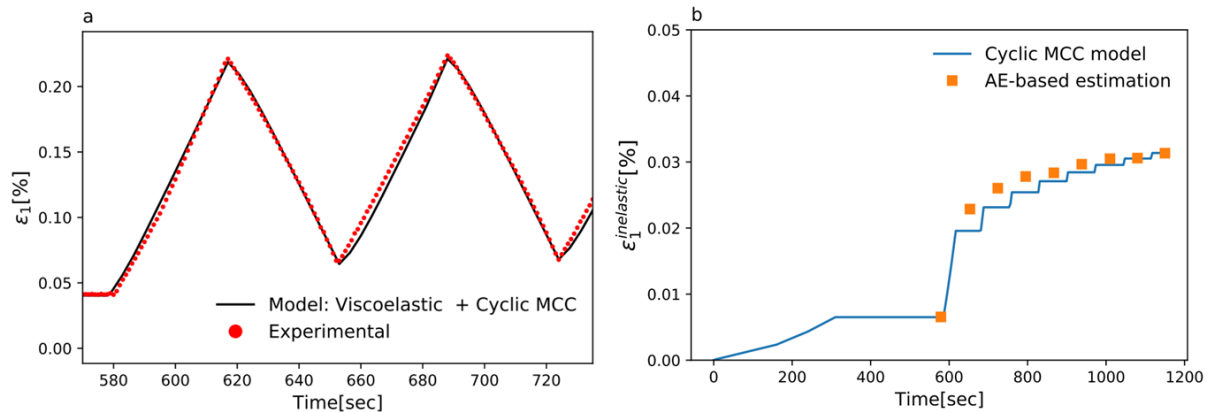


**Figure 5** The proposed model captures the non-linear strain behaviour of the experimental test (a). Response of the  $MCC_{cyclic}$  model against experimental cumulative inelastic strains (b).

## Conclusions

Interpretation of cyclic loading tests on Red felder sandstone suggests that elastic, viscoelastic and cyclic plastic deformations are taking place below the brittle yield point. Fatigue was not registered under the number of cycles tested. In fact, decreasing inelastic strains with respect to the number of cycles were measured. For modeling these deformations, a three-parameter Kelvin-Voigt model was used for the elastic strains and an extension of the Modified Cam-clay model was proposed for the cyclic inelastic strains. This work will help in quantifying the impact of inelastic strain on UES's geomechanics response in sandstones.

## References

- Carter, J. P., Booker, J., & Wroth, C. (1979). A critical state model for cyclic loading. Department of Civil Engineering, University of Queensland.
- Cerfontaine, B., Charlier, R., Collin, F., & Taiebat, M. (2017). Validation of a new elastoplastic constitutive model dedicated to the cyclic behaviour of brittle rock materials. *Rock Mechanics and Rock Engineering*, 50, 2677–2694.
- Cerfontaine, B., & Collin, F. (2018). Cyclic and fatigue behaviour of rock materials: Review, interpretation and research perspectives. *Rock Mechanics and Rock Engineering*, 51, 391–414.
- Dietl, C., Braun, R., Baumgartner, H., & Rudolph, E. (2018). Complex petrophysical studies to evaluate the safety of an underground gas storage in porous rocks. *AAPG Search and Discovery article 80642*.
- Heinemann, N. et al. (2021). Enabling large-scale hydrogen storage in porous media – the scientific challenges. *Energy Environmental Science*, 14, 853.
- Lockner, D. (1993). The role of acoustic emission in the study of rock fracture. *International Journal of Rock Mechanics and Mining Sciences Geomechanics Abstracts*, 30 (7), 883–899.
- Snijders A. (2000) Lessons from 100 ATEs projects - The developments of aquifer storage in the Netherlands TERRASTOCK 2000, Stuttgart, Germany.
- Tek, M. (1987). *Underground gas storage of natural gas (First)*. Gulf publishing company.
- Vermeer, P., & de Borst, R. (1984). Non-associated plasticity for soils, concrete and rocks. *HERON*, 124.